

Fabrication of a Biodegradable Implant with Tunable Characteristics for Bone Implant Applications

Iman Manavitehrani,[†] Ali Fathi,[†] Yiwei Wang,[‡] Peter K. Maitz,^{‡,§} Farid Mirmohseni,^{†,||} Tegan L. Cheng,^{||} Lauren Peacock,^{||} David G. Little,^{||,⊥} Aaron Schindeler,^{||,⊥} and Fariba Dehghani^{*,†,Ⓢ}

[†]The University of Sydney, School of Chemical and Biomolecular Engineering, Sydney, 2006, Australia

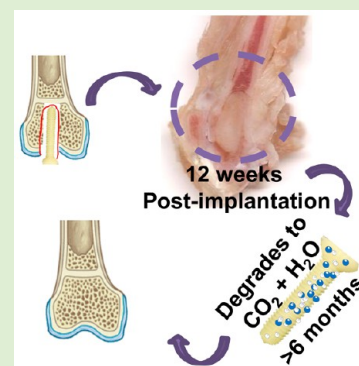
[‡]Burns Research Group, ANZAC Research Institute, University of Sydney, Concord, New South Wales 2139, Australia

[§]Burns and Reconstructive Surgery Unit, Concord Repatriation General Hospital, Concord, New South Wales 2139, Australia

^{||}Orthopaedic Research and Biotechnology, The Children's Hospital at Westmead, Westmead, 2145, Australia

[⊥]Paediatrics and Child Health, University of Sydney, Sydney, 2006, Australia

ABSTRACT: Biodegradable polymers are appealing material for the manufacturing of surgical implants as such implants break down in vivo, negating the need for a subsequent operation for removal. Many biocompatible polymers produce acidic breakdown products that can lead to localized inflammation and osteolysis. This study assesses the feasibility of fabricating implants out of poly(propylene carbonate) (PPC)–starch that degrades into CO₂ and water. The basic compression modulus of PPC–starch (1:1 w/w) is 34 MPa; however, the addition of glycerol (1% w/w) and water as plasticizers doubles this value and enhances the surface wettability. The bioactivity and stiffness of PPC–starch blends is increased by the addition of bioglass microparticles (10% w/w) as shown by in vitro osteoblast differentiation assay and mechanical testing. MicroCT analysis confirms that the bioglass microparticles are evenly distributed throughout biomaterial. PPC–starch–bioglass was tested in vivo in two animal models. A murine subcutaneous pellet degradation assay demonstrates that the PPC–starch–bioglass blend's volume fraction loss is 46% after 6 months postsurgery, while it is 27% for poly(lactic acid). In a rat knee implantation model, PPC–starch–bioglass screws inserted into the distal femur show osseointegration with no localized adverse effects after 3 and 12 weeks. These data support the further development of PPC–starch–bioglass as a medical biomaterial.



1. INTRODUCTION

Biodegradable synthetic polymers are attractive for use in tissue engineering, drug delivery, and medical implant devices.^{1–5} Compared to permanent implants made from metal or nondegradable polymers, resorbable biomaterial implants do not require a secondary operation to remove.⁶ A limited subset of biodegradable, biocompatible polymers have regulatory approval for human clinical usage. Several of the most commonly used polymers such as poly(lactic acid) (PLA) and poly(lactic-glycolic acid) (PLGA) break down to form acidic byproducts. This can lead to local cellular necrosis and bone resorption,^{7–9} which remains a significant challenge for clinical applications.¹⁰ A composite material of poly(propylene carbonate) (PPC) and starch that has a biologically benign degradation products could be superior to the current standards.¹¹

PPC–starch blends have already undergone considerable optimization in preclinical development.¹¹ Starch fillers have previously been shown to improve the amphiphilicity of biodegradable polymers such as poly(ϵ -caprolactone).¹² However, the major hurdle for the medical application of studied PPC–starch composites is the surface hydrophobic property (water contact angle of $76.45 \pm 1.30^\circ$) that can impair cell adhesion.^{13,14} In addition, the hydrophobicity of an implant may restrict or delay cell growth, migration, and ultimately the tissue

regeneration.^{15–17} Hydrophilic plasticizers such as water, oligosaccharides, polyols, and lipids have been shown to improve the surface hydrophilicity and plasticity of different polymer mixtures.¹⁸ The addition of these plasticizers might improve the bioactivity and biocompatibility of PPC–starch.

Ceramic materials such as hydroxyapatite (HA), calcium phosphates, and silica (SiO₂) based bioactive glass have all been used alone or as coatings for orthopedic implants.^{19,20} The addition of bioceramics typically enhances osseointegration, such as the addition of plasma-sprayed HA onto implants in a canine segmental femoral defect model.²¹ However, in practice, the loosening of the HA or calcium phosphate layers have been problematic in some clinical trials.^{22–24} The incorporation of ceramic microparticles into PPC–starch could improve bioactivity and reduce malleability without creating a surface that could separate in vivo.

The aim of this study was to assess for the first time the feasibility of using a PPC–starch blend in an orthopedic setting to validate the utility of this biomaterial. We hypothesized that the combination of these biodegradable polymers with bioglass

Received: January 16, 2017

Revised: April 17, 2017

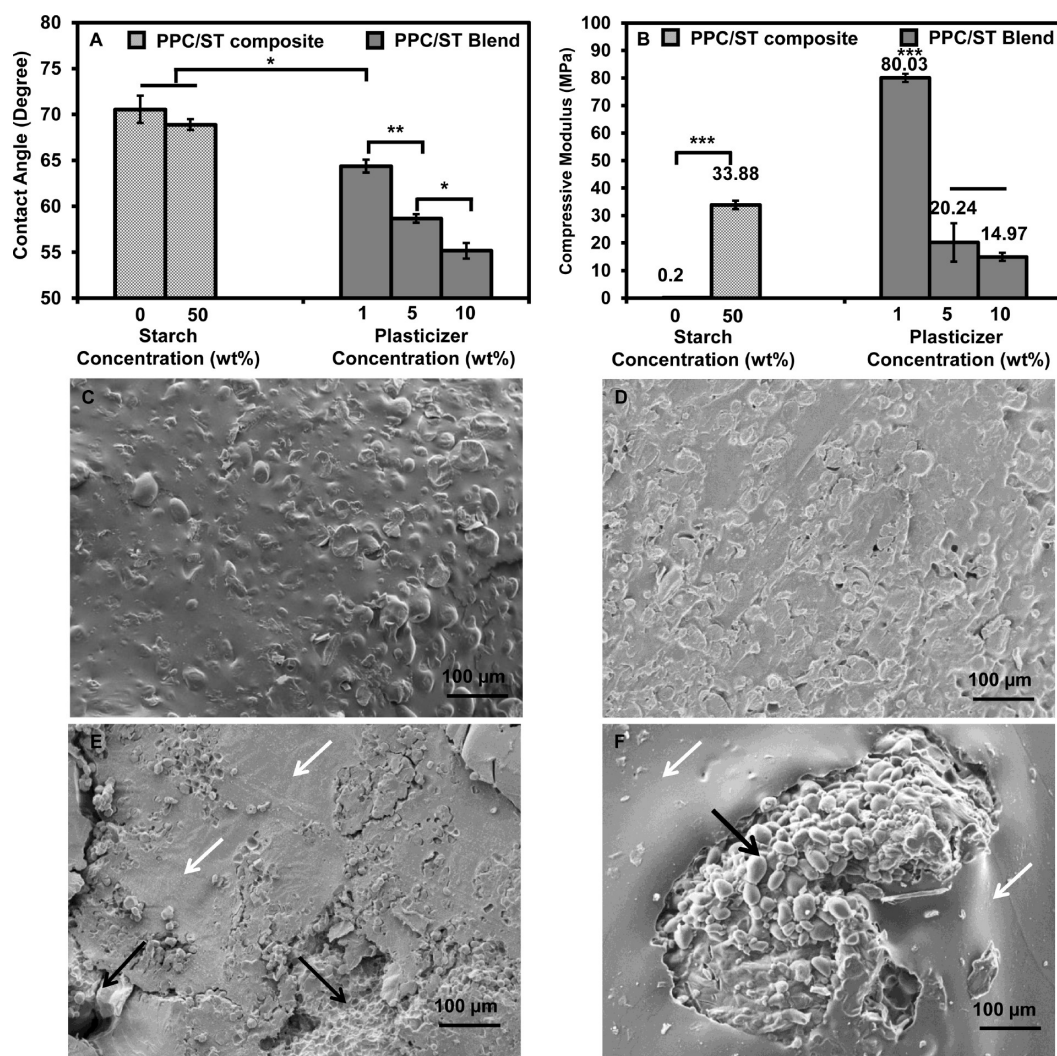


Figure 1. Effect of plasticizers on (A) contact angle measurement and (B) the compressive modulus of the PPC–starch (PPC/ST) that was blended with different plasticizer concentration (* $p < 0.05$, ** $p < 0.01$, and *** $p < 0.001$). The contact angle test was carried out using water drops. The SEM images of PPC/ST composite (C) and blends containing 1% (D), 5% (E), and 10% (F) (w/w) plasticizers. Scale bar = 100 μm . The white and black arrows are referring to PPC and starch phases, respectively.

could produce a superior biomaterial that addresses the shortfalls of currently available polymers. To this end, a hot melt compression technique was developed for the preparation of these blends. The physical properties of the blend such as compressive modulus and surface wettability were optimized using different concentrations of hydrophilic plasticizers and bioglass. Finally, in vitro testing was performed to examine osteoblast cell adhesion to these materials, while in vivo tests were conducted to compare their biodegradation and osseointegration with PLA.

2. EXPERIMENTAL SECTION

2.1. Materials. Poly(propylene carbonate) was supplied by Human Global Capital Pty Ltd. with the molecular weight (M_w) of 160 kDa. Microparticles of soluble starch ($\sim 25 \mu\text{m}$; ACS reagents), phosphate buffer saline (PBS, pH 7.4), tetraethyl orthosilicate (TEOS), β -tricalcium phosphate (puriss. p.a., $\geq 98\%$), poly(D,L-lactide) IV 0.49 dL/g (average M_w 75–120 kDa), trimethyl phosphate, McCoy's 5A medium modified, and trypsin were purchased from Sigma-Aldrich and were used without any further purification unless explicitly mentioned. Simulated body fluid (SBF, pH 7.42) was prepared based on the method described by Kokubo et al.²⁵ Briefly, 8.035 g of sodium chloride, 0.072 g of sodium sulfate (Merck Chemicals), 0.225 g of potassium chloride, 0.292 g of calcium chloride (Silform Chemicals), 0.355 g of sodium

bicarbonate, 0.231 g of potassium phosphate dibasic, and 0.311 g of magnesium chloride (Sigma-Aldrich) were dissolved in deionized water at 36 °C and the pH was adjusted between 7.42 and 7.45 by the addition of Tris (Plus one) and 1 M solution of hydrochloric acid (HCl 32%, Merck Chemical). All these chemicals and reagents were used without further purification. Alkaline phosphate assay kit was purchased from Abnova. Fetal bovine serum, L-glutamine, and antibiotic-antimycotic were obtained from Life Technologies. [3-(4,5-Dimethylthiazol-2-yl)-5-(3-carboxymethoxyphenyl)-2-(4-sulfophenyl)-2H-tetrazolium] was purchased from Promega for the MTS assays.

2.2. Fabrication of Bioglass. The bioglass microparticles were prepared via a sol–gel method described previously by our research group.²⁰ In summary, TEOS, deionized water, and HCl (100:800:1 molar ratio) were vigorously stirred for 30 min to obtain a clear solution. Known amounts of calcium chloride dihydrate and trimethyl phosphate as calcium and phosphorus sources for the preparation of sol–gel derived bioglass were used. This solution was kept in a sealed container for a few days to obtain a gel. Thermal sintering using a furnace at 700 °C was carried out to prepare a fine powder of the bioactive glass, followed by ball milling (Mikro-Dismembrator U from Sartorius Co.) to acquire desired ceramic particle size using 2000 rpm speed for 2 min. The average particle size measured using a Malvern mastersizer.

2.3. Fabrication of Polymer Blends. PPC and starch with a ratio of 1:1 (w/w) were thoroughly mixed at 170 °C for 10 min in a

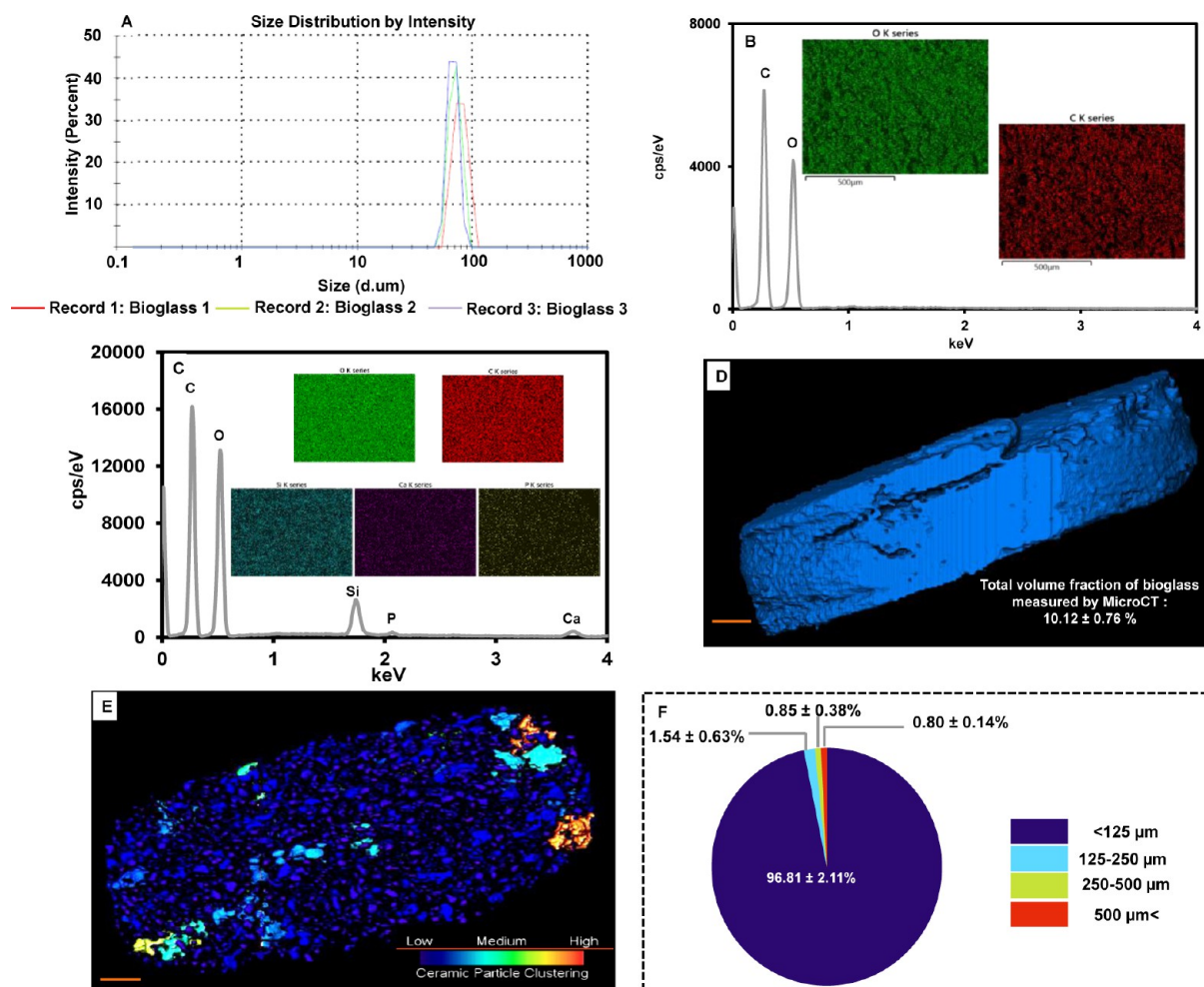


Figure 2. (A) Particle size analysis of the bioglass microparticles (3 repetitions); (B, C) SEM-EDS scans of the PPC–starch (PPC/ST) and PPC–starch–bioglass (PPC/ST/BG) blends, respectively; (D) reconstructed images of the PPC/ST/BG using 10% (w/w) of bioglass microparticles via microCT scanning; (E) the false color diagram obtained via microCT scanning marking ceramic particles with higher optical densities; (F) the clustering amount of ceramic microparticles inside the polymer ceramic blend; scale bar is 250 μm .

custom-made stainless steel vessel using a stirrer (WiseStir HS30D stirrer) at a rotation speed of 300 rpm as described previously by our research group.¹¹ The resulting paste was then placed in a custom-made cylindrically shaped mold with 1 cm in diameter and 10 cm in length. The temperature was slowly decreased to ambient conditions (25 °C), and the sample was stored at room temperature for further characterizations. Polymer blends were produced using hydrophobic plasticizers, water, and glycerol, at ratios ranging from 0 to 10% (w/w). Subsequently, a polymer blend with the 1% (w/w) plasticizer was mixed with ceramic content between 0 and 10% (w/w) for additional comparisons. Screws were manufactured in a prewarmed custom-made screw mold, and 5 tonnes force was applied to shape the screw. A similar process was performed to form PLA and PLA/calcium phosphate (CaP) screws with a composition of 70% PLA:30% CaP (w/w).²⁶ Aseptic conditions were used for in vitro and in vivo animal studies.

2.4. Contact Angle Measurement. Surface wettability of the samples was evaluated by static contact angle measurement (Ramehart Instrument). Contact angle measurements for water were performed at room temperature from the droplet image using the tangent method. Three solid flat disks of polymer blends were used to estimate the correct mean and standard deviation.

2.5. Compression and Bending Test. The mechanical strength of samples was measured using uniaxial compression tests in an unconfined state by Instron (Model 5543) with a 1000N load cell using the method described in our previous study.²⁷ The compression (mm) and load (N) were obtained at a crosshead speed of 30 $\mu\text{m s}^{-1}$ and up to 0.3 mm mm^{-1} of strain level. The compressive modulus was then calculated as the

tangent slope of stress–strain curves in the linear strain region of 0.1 to 0.2 mm $\cdot\text{mm}^{-1}$. Furthermore, the maximum load (N) and deflection at failure (mm) were tested with the same load cell using the four points bending jigs by Instron (Model 5944).

2.6. Microcomputed Tomography (MicroCT). PPC–starch–bioglass specimens were scanned with a microfocus X-ray source using Skyscan 1072 Micro-Computed Tomography scanner (Bruker Corp). During scanning, the specimen was rotated in small increments over 360 °C, and an X-ray projection image was captured at each step with the source voltage and source current equal to 58 kV and 100 μA , respectively with the image pixel size of 11.83 μm and 295 ms exposure. The 3D volumes and the false color images were generated using Avizo 3D (FEI Visualization Sciences Group originally designed and developed by the Visualization and Data Analysis Group at Zuse Institute Berlin (ZIB) under the name Amira) software.

In the knee implantation model, femora containing PPC–starch–bioglass and PLA–calcium phosphate implants were scanned using a Skyscan 1174 (Bruker Corp). Bones were scanned at an isotropic voxel resolution of 14 μm with a 0.5 mm aluminum filter, 50 kV X-ray tube voltage, 800 μA tube electric current, and 4500 ms scanning exposure time. A cutoff for mineralized tissue of 0.3 g cm^{-3} mineral was used for 3D reconstruction using NRecon software.

2.7. Scanning Electron Microscopy with Energy-Dispersive X-ray Spectroscopy (SEM-EDS). As an indication of biocompatibility, specimens were incubated with SBF at 37 °C for up to 28 days. The collected samples were washed twice with milli-Q water to remove the precipitated salts. The formation of calcium phosphate layer on the

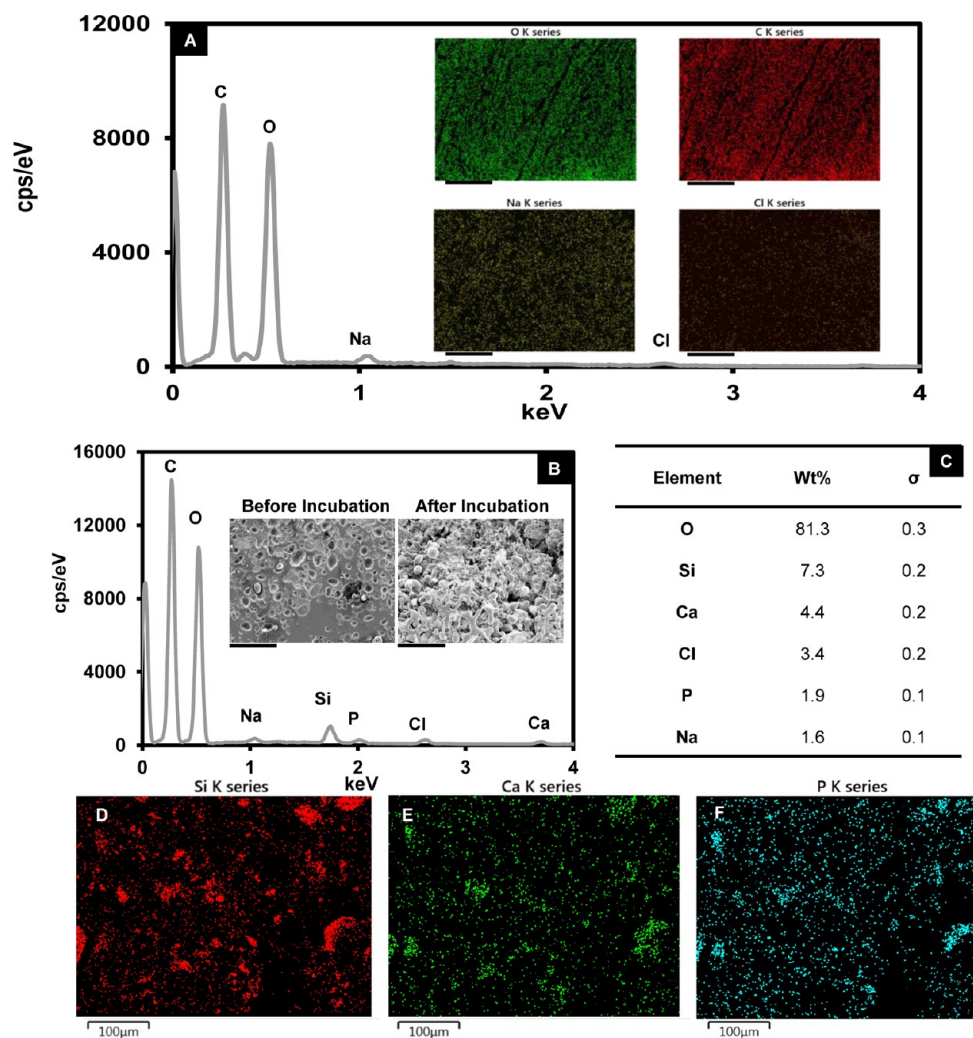


Figure 3. EDS spectra for the blend of PPC–starch (A) and PPC–starch with 10% (w/w) bioglass (B) incubated in SBF for a period of 28 days; (C) The composition of the scanned spot of the surface of the sample; (D–F) The distribution maps of the Si, Ca, and P ions on the surface of the blend (scale bar is 250 μm for panel A and 100 μm for panel B).

surface of the sample incubated in SBF was examined by Zeiss EVO 50 SEM, operating at an acceleration voltage of 10 kV fitted with a LaB6 filament. Routine EDS measurements are possible using an iXRF Iridium Ultra EDS system. The AZtec software (Oxford Instruments, U.K.) was integrated into SEM device to identify the chemical composition of polymer ceramic implants. The samples were mounted on aluminum stubs using conductive silver paint, and then carbon coated before SEM analysis.

2.8. Osteoblast Culture and Functional Assays. The Saos-2 cells (Sarcoma osteogenic) attachment on the surface of the specimens was measured at different time intervals within 28 days postculture. Sterile samples were placed in 24-well plates, and 75 μL of cell suspension was added to each well for a total of 2×10^5 cells/well. The primary and secondary fixatives (2.5% glutaraldehyde and 1% osmium tetroxide in 0.1 M PBS) were used to fix the cells for an hour followed by three PBS washes at room temperature. Sequential dehydration using 30%, 50%, 70%, 90%, and pure ethanol was performed. This was followed by treatment with 0.5 mL of hexamethyldisilazane (HMDS) for 2 min at room temperature in a desiccator to eliminate ethanol residue. Samples were mounted on aluminum stubs using conductive carbon paint, then gold coated by using an Emitech K7550X instrument for SEM analysis.

Samples fabricated in aseptic conditions were placed in 24-well plates, and 50 μL of Saos-2 (Sarcoma osteogenic) cell suspension was added to each well to reach the initial cell count of 2×10^5 per well plate. Cell viability test was studied by using the MTS assay at different time points,

for example, 1, 3, and 7 days postculture. At each time point, old media removed from the wells followed by three times PBS washing. Then, samples soaked in 250 μL of fresh media and 50 μL of MTS solution for 1 h at 37 $^\circ\text{C}$ incubator. The viability of cells was quantified by measuring the absorbance of the resulting solutions at 490 nm wavenumbers.

The differentiation of Saos-2 cells was determined using alkaline phosphate assay (ALP) as an osteogenic marker.²⁸ After 14, 21, and 28 days postculture, the cells were trypsinized from the surface of samples, and their ALP activities were evaluated based on manufacture's procedure. The ALP activity of cells was quantified by measuring the absorbance of the resulting solutions at 415 nm wavenumbers with a microplate reader (Bio-Rad 680).

2.9. In Vivo Degradation. A mouse subcutaneous implantation model was used with pathogen-free male and female Balb/c mice, aged 12 weeks and weighing 25 ± 1.7 g (male) and 22 ± 1.2 (female). Animals were housed (19–22 $^\circ\text{C}$, 12 h light, 12 h dark cycle) in cages with unrestricted access to food and water. Procedures were approved by SLHD Animal Welfare Committee Australia (AWC NO.2013/019B). Each mouse ($n = 12$) was anesthetized individually by intraperitoneal injection of a mixture of ketamine (75 mg mL^{-1}) and xylazine (10 mg mL^{-1}) at 0.01 mL g^{-1} of body weight. The dorsal hair was shaved; the skin was cleaned with betadine solution and washed with sterile saline. Four adjacent but identical incisions were created surgically in the dorsal area to create a subcutaneous pouch. The PPC–starch, PPC–starch–bioglass, and PLA screws were inserted before closing with 5–0 silk sutures and covering by Atrauman (Hartmann,

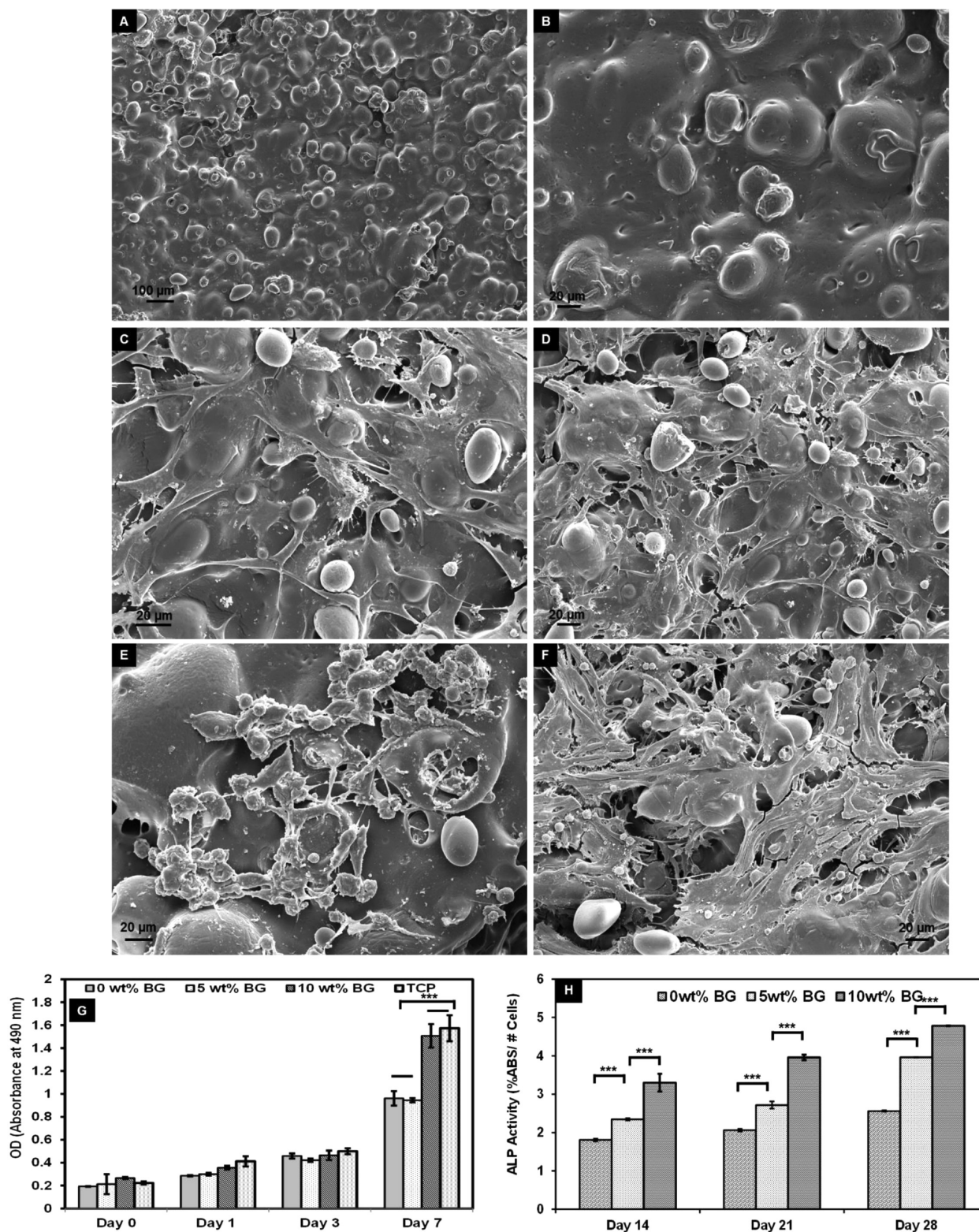


Figure 4. SEM micrographs of PPC–starch–bioglass (PPC/ST/BG) blends with different magnifications before the cell incubation (A, B); Osteoblast cells cultured on surfaces of the PPC–starch (PPC/ST) and PPC/ST/BG blends after 1 day (C, D) and 3 days (E, F), respectively. (G) Cytotoxicity test from MTS assay. (H) Alkaline phosphate activity of the osteoblast cells after 14, 21, and 28 days containing different amount of bioglass microparticles (** $p < 0.001$).

Australia) and IV3000 wound dressings (Smith and Nephew) for 7 days. Carprofen (5 mg kg^{-1}) was given at the time of anesthesia and following 2 days postsurgery for analgesia. After surgery, mice were caged individually for the first 2 days and then 3 mice per cage thereafter with free access to water and food. Biopsies were collected for MicroCT analysis

at 4, 12, and 24 weeks postimplantation. Biopsies were fixed in 10% formalin for 24 h.

2.10. Osseointegration Study. A knee implantation model was performed in 15+ weeks old male Wistar Rats (Animal Resources Centre). In brief, animals were anesthetized with ketamine/xylazine

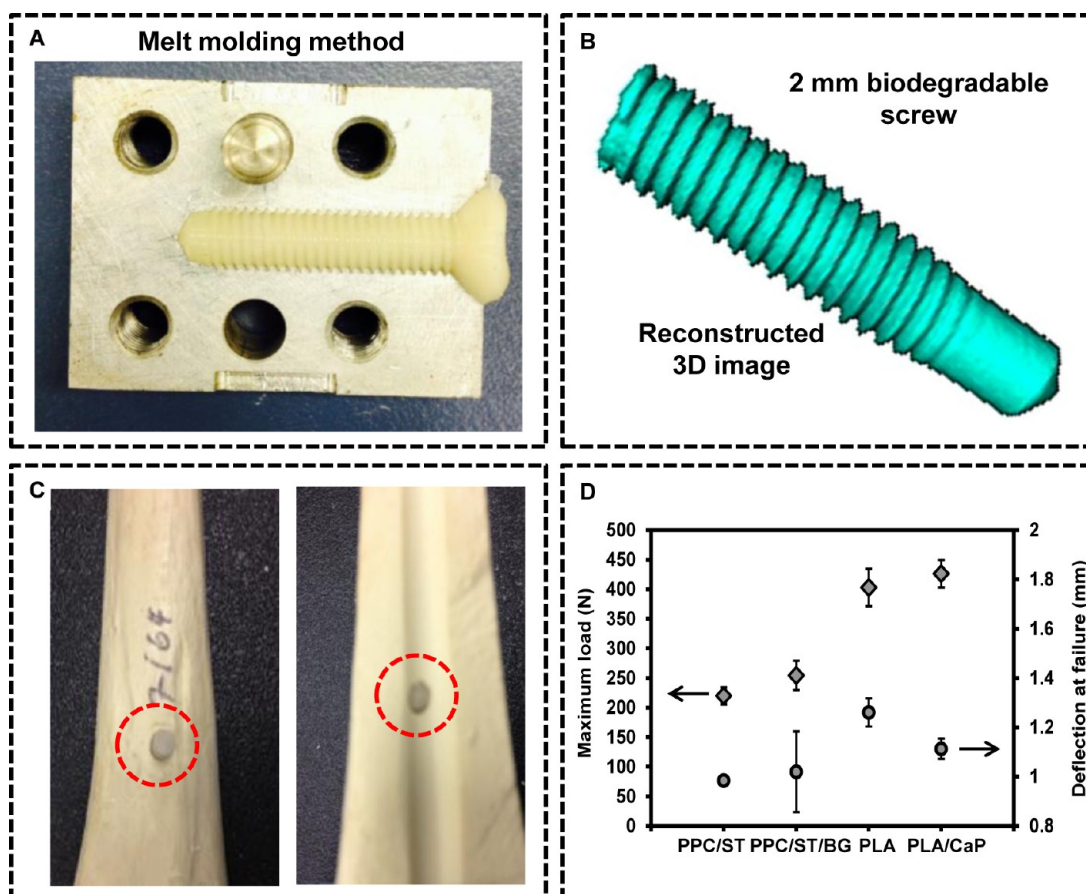


Figure 5. Biodegradable screw made via melt blending method (A), visualized after 3D scanning with microcomputed tomography and reconstruction with Avizo software (B). The screw was placed into a synthetic bone drilled with drill bit number 7/64 in. (C). (D) Maximum bending load and deflection at the failure of the polymer ceramic blends.

(75 mg kg⁻¹/10 mg kg⁻¹). A single incision was made at the knee, and a hole was drilled into the distal femur. Implants (PLA–calcium phosphate and PPC–starch–bioglass) were press-fit, and the surgical site closed using Vicryl suture. Animals were monitored and given 0.1 mg kg⁻¹ buprenorphine up to every 12 h for pain relief. The experimental end points were at 3 and 12 weeks ($n = 4$ per group per time point). Outcome measures included an X-ray (Faxitron), microCT (Skyscan 1174), and histological appearance following bisection with a diamond saw. Histological sections were performed on specimens decalcified for 10 weeks, embedded in paraffin, and stained with Picrosirius Red and Alcian Blue. The quantitative evaluation of newly formed bone on PLA versus PPC/ST/BG samples was performed using ImageJ analysis (Image, Adjust, Color Threshold, RGB mode (Red 161, Green 171, and Blue 201)). In this method, the sample position offset by 1 mm and the newly formed bone measured using the covered surface area. The method was also validated using conventional Freehand selection in ImageJ software with significantly no different results.

2.11. Statistical Analysis. Results of contact angle measurements, mechanical properties, ALP activity, and degradation rate calculations were reported as mean \pm SD, acquired from at least three independent experiments in each condition. Statistical significance was tested using a one-way analysis of variance (ANOVA). The statistical method used in evaluating the amount of new bone were an unpaired t test using a statistical significance alpha < 0.05 .

3. RESULTS AND DISCUSSION

3.1. Addition of Plasticizer in the PPC–Starch Blending Process. Despite prior data showing that starch can enhance the hydrophilic properties of hydrophobic polymers,¹² we observed no difference between PPC and PPC–starch in contact angle

measurements (Figure 1A). Thus, in an attempt to alter the amphiphilicity of the material, different plasticizers were used to supplement the blend.

The impact of adding water/glycerol (1:1 v/v) was tested by measuring surface contact angle. Increasing the amount of plasticizer significantly enhanced the surface wettability of PPC–starch samples (Figure 1A). The surface amphiphilicity values were increased after using 1%, 5%, and 10% water/glycerol (w/w) from 68.9 ± 0.58 (no plasticizer) to 64.37 ± 0.7 , 58.67 ± 0.46 , and $55.15 \pm 0.85^\circ$, respectively. Decreasing the contact angle was anticipated to enhance the in vivo biocompatibility of the material.²⁹

The addition of plasticizer also had a significant impact on the compressive modulus of the PPC–starch blend (Figure 1B). Using 1% water/glycerol (w/w) increased the compressive modulus of the PPC–starch blend from 33.88 ± 1.51 to 80.03 ± 6.98 MPa due to the enhanced miscibility of PPC matrix with starch as a filler.^{30,31} However, further increases of plasticizer at 5% and 10% (w/w) dramatically decreased the compressive modulus of the PPC–starch blend. Similar behavior was also observed in the study by Jost et al. using glycerol and sorbitol.³² This phenomenon was attributed to the phase separation at higher concentrations of plasticizer. Heterogeneous aggregates are observed in SEM images with 5% and 10% (w/w) plasticizer (Figure 1C–F). Thus, the 1% water/glycerol value was used for subsequent experiments and the samples were noted as PPC/ST.

Hydrophilic plasticizers such as water, polyols, and oligosaccharides are broadly used to enhance the surface wettability.

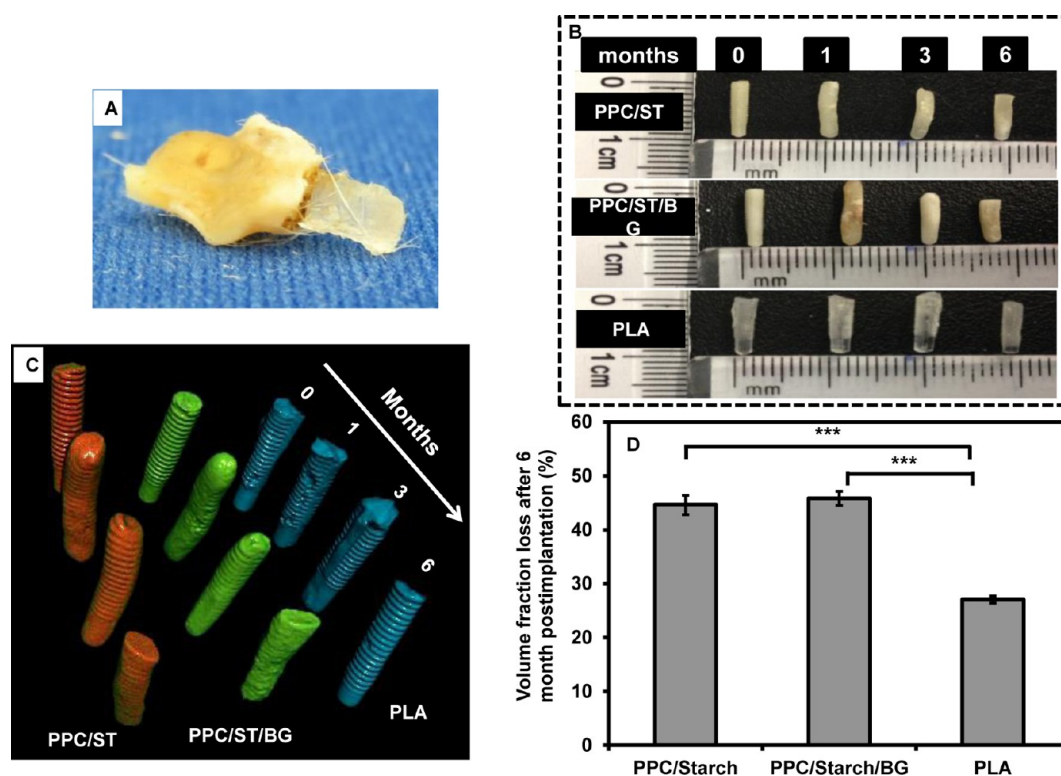


Figure 6. (A) Bitten off PLA screw that rejected by mice a month after surgery. (B) Appearance of the implants before and after 1, 3, and 6 months surgery. (C) Reconstructed images of the implanted screws visualized by X-ray scanning tomography. (D) Volume fraction loss (%) after 6 months postimplantation.

They can also facilitate the processing of polymer blends due to their low molecular weight and stability.^{33,34} These compounds act as agents that promote intermolecular interaction between PPC (hydrophobic) and starch (hydrophilic), therefore enhance the miscibility between these two polymers. Our data is consistent with prior reports showing that plasticizers can promote the surface properties and wettability of hydrophobic polymer–starch blends.^{35,36}

3.2. Addition of Bioglass to the PPC–Starch Blend. A melt blending method was used to prepare a homogeneous mixture of bioglass in PPC–starch blends. The bioglass particles employed in this study had an average particles size of 100 μm . These particles were uniformly distributed in the polymer matrix by the manufacturing process used and minimally agglomerated as shown in Figure 2A–C. In preliminary studies by us (data not shown) and others,³⁷ addition of >10% bioglass (w/w) to the polymer–bioglass blends formed brittle structures; thus, higher amounts were not utilized in subsequent studies. Furthermore, the water contact angle measurement after addition of bioglass microparticles showed no significant difference in surface wettability.

The calcium and phosphate ions that loaded into the silica network via thermal sintering remained inside the structure. Furthermore, the distribution of ceramic microparticles inside the polymer blend matrix was visualized by microCT to validate the homogeneity of the structure (Figure 2D,E) in false color images. More than $96.81 \pm 2.11\%$ of the bioglass aggregates in the PPC–starch–bioglass implants were less than 125 μm ; this was comparable to the average particle size of ceramic powders (100 μm) used for blending. Quantification showed that the total volume of the agglomerated particles was less than 4% (Figure 2F). The precision of this method was validated by

calculating the total volume of the ceramic particles measured by microCT, which gave a value of $10.12 \pm 0.76\%$; equivalent to the 10% (w/w), which was measured and added.

Bioglass micro- and nanoparticles have been previously used to enhance the bioactivity and biocompatibility of bone implants.^{38–40} While we have used a single size of bioglass particles, other groups have shown that bioactivity measures can be augmented by decreasing particle size.²⁰ It has been speculated that this relationship is related to particle surface area, thus implying that agglomeration (which would reduce surface area) would be unfavorable.

3.3. In Vitro Properties of PPC–Starch–Bioglass. To recapitulate the conditions that an implant would be exposed to in a biological/medical setting, samples were incubated for 28 days in simulated body fluid (SBF). The polymer blend was unable to promote the de novo formation of a hydroxyapatite layer featuring calcium and phosphorus on the specimen surface (Figure 3A). In contrast, the addition of bioglass microparticles did yield calcium and phosphorus as detected by EDS that eluted from the implant surface (Figure 3B–F). The ratio between the calcium and phosphate ions (Ca/P) was calculated to be 1.52 ± 0.07 . Notably, a Ca/P ratio between 1.50 and 1.667 corresponds to the hydroxyapatite structure with the highest ability to regenerate bone tissue.⁴¹ This ratio was calculated considering the Ca, P signals from bioglass in the underlying substrate followed by subtraction from the values after SBF incubation.

Using an in vitro culture system, cell adhesiveness of Saos-2 osteoblasts was measured on the surface of PPC-starch with and without 10% bioglass (w/w). Cell adhesion was visualized using SEM imaging (Figure 4A–F). Both polymer blends with and without bioglass resulted in osteoblasts adhering at day 1 and showing a flattened morphology after 3 days.

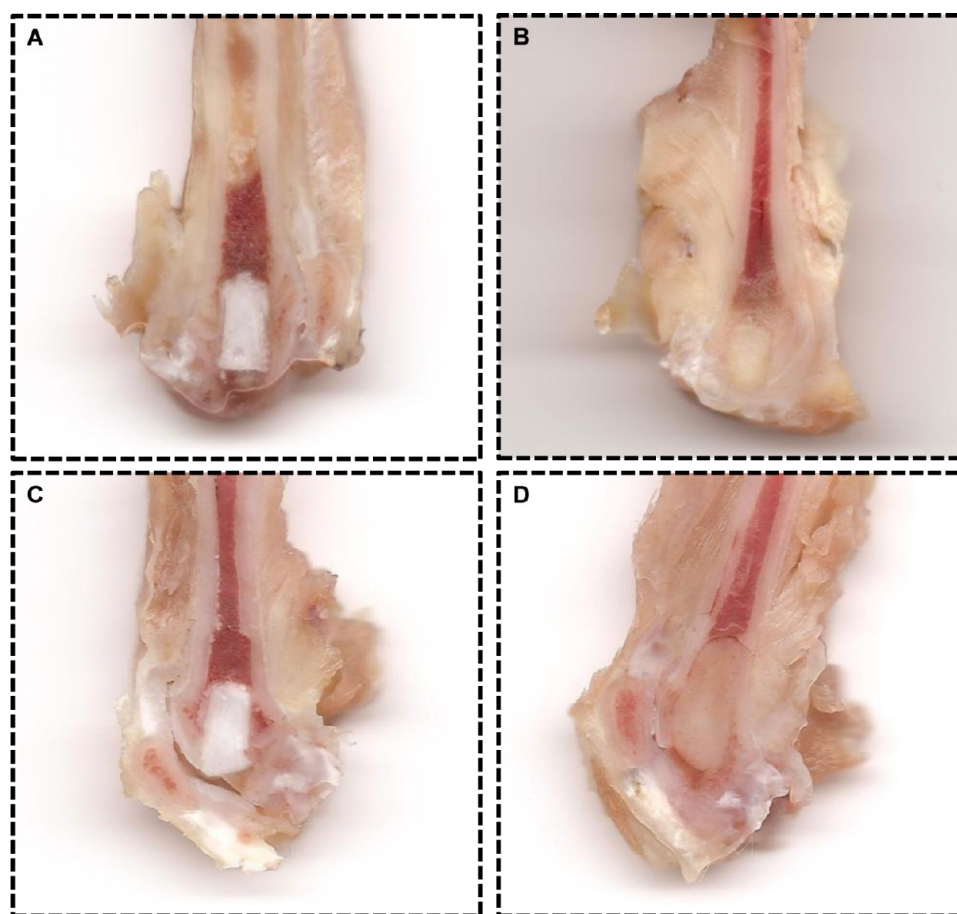


Figure 7. Representative images of bisected distal femora containing polymer implants inserted into the knee in a rat model. PLA–calcium phosphate (A, C) and PPC–starch–bioglass (B, D) implants were compared at 3 weeks (A, B) and 12 weeks (C, D). The majority of both implant types remained at 12 weeks. The PPC–starch–bioglass samples showed evidence of swelling.

The osteoblastic differentiation ability of the samples was studied by alkaline phosphatase (ALP) assays after 28 days (Figure 4H). Osteoblastic differentiation is required for new bone formation and may yield superior outcomes in an orthopedic setting.⁴² The ALP activity was found to increase in proportion to the amount of bioglass (0%, 5%, and 10% w/w) included in the blend. ALP data was normalized to cell number, as measured by MTS assay (Figure 4G). These data are consistent with prior findings that PPC promotes cell attachment and is biocompatible.^{43,44}

3.4. Fabrication of Biodegradable Screw. One potential application for the PPC–starch–bioglass material was biodegradable screws that could be used for orthopedic applications. Screws were fabricated using a melt molding method (Figure 5A,B). Well structurally defined screws could be fabricated by melt mixing using the optimized 1:1 ratio of PPC and starch, 1% plasticizers, and 10% bioglass at 170 °C.

Screws were tested in principle via insertion into a synthetic bone. Polymer screws could be readily implanted (Figure 5C). Subsequently, four points bending tests were performed to measure the maximum load and deflection at the failure of screws (Figure 5D). The deflection scores showed no significant differences with the addition of ceramic microparticles, and the low to average deflection values suggest that the screws have a brittle structure. This is consistent with the findings of Halász et al.⁴⁵ The maximum tolerated loads at the failure points showed similar trends.

3.5. Biodegradation of Polymer Screws in a Subcutaneous Implantation Model. The in vivo degradation rate of the biodegradable screw was measured to estimate the stability of the screws in the body. The screws were implanted subcutaneously in mice, and the volume of each sample was calculated after 1, 3, and 6 months postsurgery. In this study, volume fraction loss was selected as a primary outcome over the loss of mass; the invasion of tissues and blood vessels into the samples can cause inaccuracy when utilizing gravimetric methods. The volume determined by microCT scanning and the invaded tissues were separated from the polymers according to optical density.

After the first month, mice who received PLA screws rejected the implants, and some rodents tried to remove the implants from their backs (illustrated in Figure 6A). This is consistent with the acidic degradation of the implant causing irritation and discomfort in the animals.^{46,47} To ameliorate this, extra wound dressings were used to cover the surgical sites. The implanted screws over 6 months postsurgery showed that the shape was largely retained over the first 3 months (Figure 6B,C).

As the degradation of implants results in the decrease of mechanical properties, they should last longer than the required regeneration time to be applicable for load-bearing applications. To this end, the volume fraction loss was measured over six months and, as expected, the bulk degradation was only significantly noted after this period. The time frame for this study is relevant to orthopedic procedures and the period required for

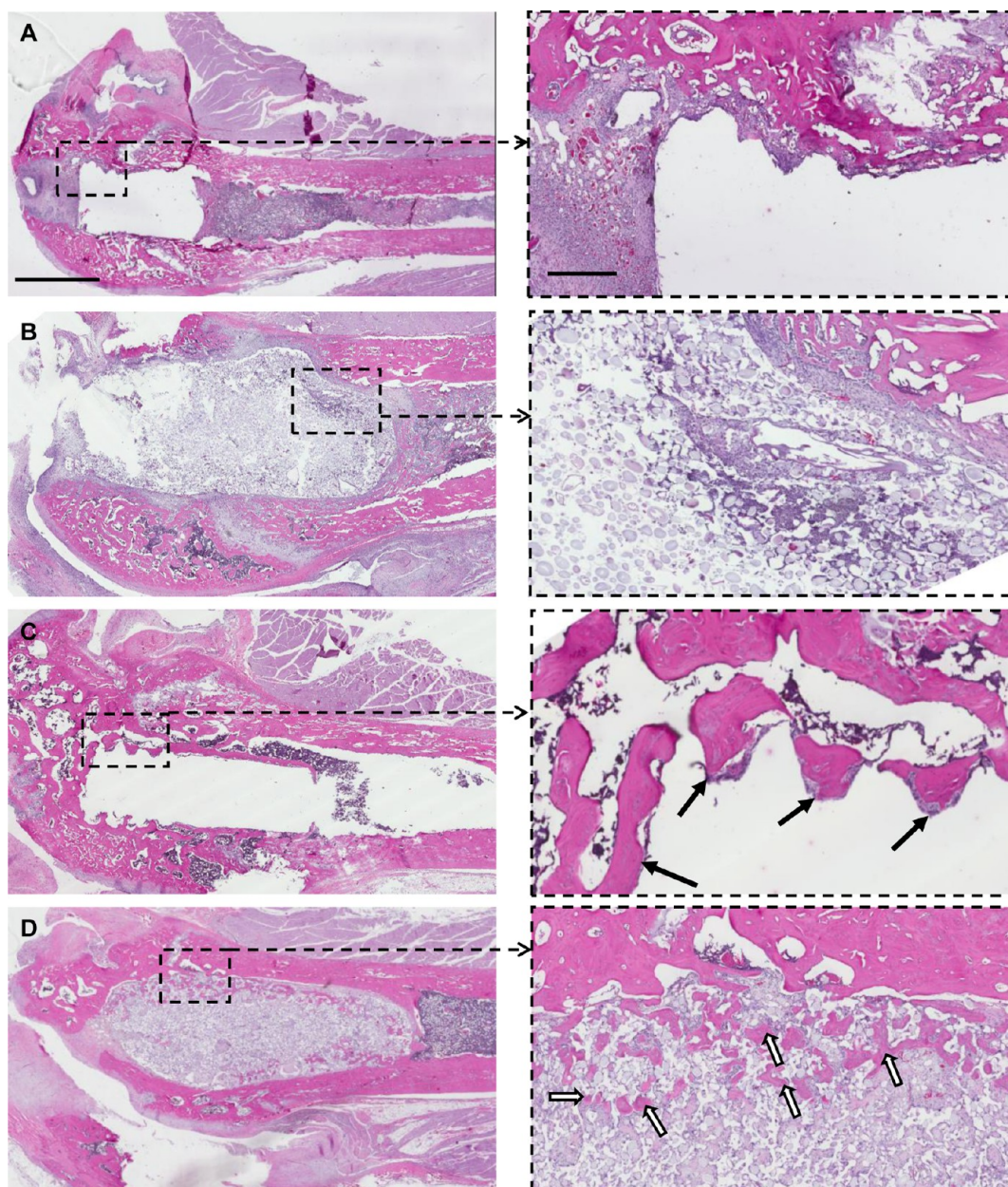


Figure 8. Hematoxylin and eosin staining of paraffin sections of the implantation site of (A, C) PLA–calcium phosphate and (B, D) PPC–starch–bioglass screws 3 and 12 weeks postimplantations, respectively. The scale bars are 3 mm (left column) and 500 μm (right column). Black arrows in the figure show the bone formed in the PLA–calcium phosphate screw threads. Black bordered white arrows indicate new bone invading the PPC–starch–bioglass.

bone remodeling postinjury.^{48,49} Conspicuously, the inclusion of bioglass did not significantly affect degradation as PPC–starch ($44.6 \pm 1.8\%$) and PPC–starch–bioglass ($45.82 \pm 1.3\%$) showed higher volume loss than PLA ($27.05 \pm 0.65\%$; Figure 6D).

3.6. In Vivo Biocompatibility and Osseointegration in a Knee Implantation Model. Polymer implants were inserted into a drill hole in the knee in a modified knee implantation model. Threaded implants were used to improve fixation and to subsequently examine implant shape, degradation, and osseointegration. Both polymers were well tolerated by the animals. One animal containing the PPC–starch–bioglass implants was prematurely culled due to unexplained weight loss, however, a postmortem revealed no cause for this and the implant site showed no signs of inflammation or infection.

The remaining specimens were harvested at 3 and 12 week time points and scanned by microCT. Reconstructed images revealed that the drill holes were not filled in at either time point (data not shown). Fixed specimens were then bisected using an orthopedic diamond saw and implants examined (Figure 7A–D). PLA samples showed minimal changes over the 12 week period and new bone was found to form by 12 weeks adjacent to the implants. In contrast, the PPC–starch–bioglass samples showed significant swelling that could be potentially attributed to the polymer–starch blend absorbing water.

Histological sections were examined from both time points (Figure 8). Notably, those specimens containing PLA were unable to retain the implant, however osseointegration was qualitatively observed by 12 weeks. There was no significant breakdown of the PLA screws over the duration of the study as

the threading was still present as shown by new bone outlining the threads (Figure 8C'). In contrast, the PPC–starch–bioglass screws were able to be sectioned. PPC–starch–bioglass implants showed evidence of a healthy cellular response at 3 weeks surrounding the implant (Figure 8B'). By 12 weeks the implants were substantively osseointegrated, with the surrounding bone starting to invade the implant (Figure 8D'). Particles of bioglass could also be seen to be evenly distributed at high magnification. In PPC/ST/BG samples, nearly $40.05 \pm 0.79\%$ of the surface of the selected area covered by new bone after 12 weeks of implantation. However, this value for PLA was calculated as $33.50 \pm 0.94\%$.

4. CONCLUSIONS

In this paper, we describe a new and efficient blending method for generating a polymer–ceramic composite utilizing PPC, starch, plasticizer agents, and bioglass. This composite was found to have enhanced physical and biological properties to conventionally described PPC–starch. The blend showed significantly higher mechanical strength and hydrophilicity, which we anticipate would be ideal for medical applications. Screws made from PPC–starch–bioglass were tested in subcutaneous and bone implantation models. The results showed that this material was well tolerated and with a moderately faster degradation profile than PLA and a greater capacity for bone ingrowth. Future studies will continue to translationally develop this material for orthopedic applications.

AUTHOR INFORMATION

Corresponding Author

*E-mail: fariba.dehghani@sydney.edu.au. Fax: +61-293512854.

ORCID

Fariba Dehghani: [0000-0002-7805-8101](https://orcid.org/0000-0002-7805-8101)

Notes

The authors declare no competing financial interest.

ACKNOWLEDGMENTS

The authors acknowledge the financial support of the Australian Research Council and Global Human Capital Pty Ltd. I.M. acknowledges the funding from the University of Sydney for the postgraduate scholarship. A.F. acknowledges the financial support from the Australian government for Australian Postgraduate Research Award Scholarship. In addition, the authors acknowledge the scientific and technical assistance of the Australian Microscopy and Microanalysis Research Facility at the Scanning Electron Microscopy and MicroCT imaging units at the University of Sydney.

REFERENCES

- (1) Ratner, B. D.; Hoffman, A. S.; Schoen, F. J.; Lemons, J. E., Introduction - Biomaterials Science: An Evolving, Multidisciplinary Endeavor. In *Biomaterials Science*, 3rd ed.; Lemons, B. D. R. S. H. J. S. E., Ed.; Academic Press, 2013; pp xxv–xxxix.
- (2) Sin, L. T.; Rahmat, Abdul, R.; Rahman, Wan, A. W. A. Applications of Poly(lactic Acid). In *Handbook of Biopolymers and Biodegradable Plastics*; Ebnesajjad, S., Ed.; William Andrew Publishing: Boston, 2013; pp 55–69.
- (3) Diaz, A.; Katsarava, R.; Puiggali, J. Synthesis, Properties and Applications of Biodegradable Polymers Derived from Diols and Dicarboxylic Acids: From Polyesters to Poly(ester amide)s. *Int. J. Mol. Sci.* **2014**, *15* (5), 7064–7123.

- (4) Sokolsky-Papkov, M.; Agashi, K.; Olaye, A.; Shakesheff, K.; Domb, A. J. Polymer carriers for drug delivery in tissue engineering. *Adv. Drug Delivery Rev.* **2007**, *59* (4–5), 187–206.

- (5) Huang, J.-N.; Jing, X.; Geng, L.-H.; Chen, B.-Y.; Mi, H.-Y.; Peng, X.-F. A novel multiple soaking temperature (MST) method to prepare polylactic acid foams with bi-modal open-pore structure and their potential in tissue engineering applications. *J. Supercrit. Fluids* **2015**, *103*, 28–37.

- (6) O'Brien, F. J. Biomaterials & scaffolds for tissue engineering. *Mater. Today* **2011**, *14* (3), 88–95.

- (7) Ding, Z. H.; Liu, Z. J.; Wei, W.; Li, Z. Y. Preparation and characterization of plla composite scaffolds by ScCO₂-induced phase separation. *Polym. Compos.* **2012**, *33* (10), 1667–1671.

- (8) Denmark, S.; Finne-Wistrand, A.; Schander, K.; Hakkarainen, M.; Arvidson, K.; Mustafa, K.; Albertsson, A. C. In vitro and in vivo degradation profile of aliphatic polyesters subjected to electron beam sterilization. *Acta Biomater.* **2011**, *7* (5), 2035–2046.

- (9) Dogan, A.; Demirci, S.; Bayir, Y.; Halici, Z.; Karakus, E.; Aydin, A.; Cadirci, E.; Albayrak, A.; Demirci, E.; Karaman, A.; Ayan, A. K.; Gundogdu, C.; Sahin, F. Boron containing poly-(lactide-co-glycolide) (PLGA) scaffolds for bone tissue engineering. *Mater. Sci. Eng., C* **2014**, *44*, 246–253.

- (10) Manavitehrani, I.; Fathi, A.; Badr, H.; Daly, S.; Negahi Shirazi, A.; Dehghani, F. Biomedical Applications of Biodegradable Polyesters. *Polymers* **2016**, *8* (1), 20.

- (11) Manavitehrani, I.; Fathi, A.; Wang, Y.; Maitz, P. K.; Dehghani, F. Reinforced Poly(Propylene Carbonate) Composite with Enhanced and Tunable Characteristics, an Alternative for Poly(lactic Acid). *ACS Appl. Mater. Interfaces* **2015**, *7* (40), 22421–22430.

- (12) Ciardelli, G.; Chiono, V.; Vozi, G.; Pracella, M.; Ahluwalia, A.; Barbani, N.; Cristallini, C.; Giusti, P. Blends of Poly-(ε-caprolactone) and Polysaccharides in Tissue Engineering Applications. *Biomacromolecules* **2005**, *6* (4), 1961–1976.

- (13) Anselme, K. Osteoblast adhesion on biomaterials. *Biomaterials* **2000**, *21* (7), 667–681.

- (14) Rebollar, E.; Frischauf, I.; Olbrich, M.; Peterbauer, T.; Hering, S.; Preiner, J.; Hinterdorfer, P.; Romanin, C.; Heitz, J. Proliferation of aligned mammalian cells on laser-nanostructured polystyrene. *Biomaterials* **2008**, *29* (12), 1796–1806.

- (15) Lee, J. H.; Lee, H. B. A Wettability Gradient as a Tool to Study Protein Adsorption and Cell-Adhesion on Polymer Surfaces. *J. Biomater. Sci., Polym. Ed.* **1993**, *4* (5), 467–481.

- (16) Allen, L. T.; Tosetto, M.; Miller, I. S.; O'Connor, D. P.; Penney, S. C.; Lynch, I.; Keenan, A. K.; Pennington, S. R.; Dawson, K. A.; Gallagher, W. M. Surface-induced changes in protein adsorption and implications for cellular phenotypic responses to surface interaction. *Biomaterials* **2006**, *27* (16), 3096–3108.

- (17) Lee, J. N.; Jiang, X.; Ryan, D.; Whitesides, G. M. Compatibility of mammalian cells on surfaces of poly(dimethylsiloxane). *Langmuir* **2004**, *20* (26), 11684–11691.

- (18) Suyatma, N. E.; Tighzert, L.; Copinet, A. Effects of hydrophilic plasticizers on mechanical, thermal, and surface properties of chitosan films. *J. Agric. Food Chem.* **2005**, *53* (10), 3950–3957.

- (19) Qian, J.; Xu, W.; Yong, X.; Jin, X.; Zhang, W. Fabrication and in vitro biocompatibility of biomorphic PLGA/nHA composite scaffolds for bone tissue engineering. *Mater. Sci. Eng., C* **2014**, *36*, 95–101.

- (20) Ravarian, R.; Zhong, X.; Barbeck, M.; Ghanaati, S.; Kirkpatrick, C. J.; Murphy, C. M.; Schindeler, A.; Chrzanowski, W.; Dehghani, F. Nanoscale Chemical Interaction Enhances the Physical Properties of Bioglass Composites. *ACS Nano* **2013**, *7* (10), 8469–8483.

- (21) Goodman, S. B.; Yao, Z.; Keeney, M.; Yang, F. The future of biologic coatings for orthopaedic implants. *Biomaterials* **2013**, *34* (13), 3174–3183.

- (22) Zhang, B. G. X.; Myers, D. E.; Wallace, G. G.; Brandt, M.; Choong, P. F. M. Bioactive Coatings for Orthopaedic Implants-Recent Trends in Development of Implant Coatings. *Int. J. Mol. Sci.* **2014**, *15* (7), 11878–11921.

- (23) Reikeras, O.; Gunderson, R. B. Failure of HA coating on a gritblasted acetabular cup - 155 patients followed for 7–10 years. *Acta Orthop. Scand.* **2002**, *73* (1), 104–108.
- (24) Mann, K. A.; Miller, M. A.; Costa, P. A.; Race, A.; Izant, T. H. Interface Micromotion of Uncemented Femoral Components from Postmortem Retrieved Total Hip Replacements. *J. Arthroplasty* **2012**, *27* (2), 238–245.
- (25) Kokubo, T.; Takadama, H. How useful is SBF in predicting in vivo bone bioactivity? *Biomaterials* **2006**, *27* (15), 2907–2915.
- (26) Antoniac, I.; Laptoiu, D.; Popescu, D.; Cotrut, C.; Parpala, R., Development of Bioabsorbable Interference Screws: How Biomaterials Composition and Clinical and Retrieval Studies Influence the Innovative Screw Design and Manufacturing Processes. *Biologically Responsive Biomaterials for Tissue Engineering*; Springer, 2013; pp 107–136.
- (27) Fathi, A.; Mithieux, S. M.; Wei, H.; Chrzanowski, W.; Valtchev, P.; Weiss, A. S.; Dehghani, F. Elastin based cell-laden injectable hydrogels with tunable gelation, mechanical and biodegradation properties. *Biomaterials* **2014**, *35* (21), 5425–5435.
- (28) Negahi Shirazi, A.; Fathi, A.; Suarez, F. G.; Wang, Y.; Maitz, P. K.; Dehghani, F.; Novel, A. Strategy for Softening Gelatin–Bioactive-Glass Hybrids. *ACS Appl. Mater. Interfaces* **2016**, *8* (3), 1676–1686.
- (29) Thankam, F. G.; Muthu, J. Alginate–polyester comonomer based hydrogels as physiochemically and biologically favorable entities for cardiac tissue engineering. *J. Colloid Interface Sci.* **2015**, *457*, 52–61.
- (30) Andersen, P. J.; Hodson, S. K. Thermoplastic starch compositions incorporating a particulate filler component. *Google Patent*, 2001.
- (31) Labouffie, F.; Hémati, M.; Lamure, A.; Diguët, S. Effect of the plasticizer on permeability, mechanical resistance and thermal behaviour of composite coating films. *Powder Technol.* **2013**, *238*, 14–19.
- (32) Jost, V.; Kobsik, K.; Schmid, M.; Noller, K. Influence of plasticiser on the barrier, mechanical and grease resistance properties of alginate cast films. *Carbohydr. Polym.* **2014**, *110*, 309–319.
- (33) Casariego, A.; Souza, B. W. S.; Vicente, A. A.; Teixeira, J. A.; Cruz, L.; Díaz, R. Chitosan coating surface properties as affected by plasticizer, surfactant and polymer concentrations in relation to the surface properties of tomato and carrot. *Food Hydrocolloids* **2008**, *22* (8), 1452–1459.
- (34) Bangyekan, C.; Aht-Ong, D.; Srikulkit, K. Preparation and properties evaluation of chitosan-coated cassava starch films. *Carbohydr. Polym.* **2006**, *63* (1), 61–71.
- (35) Gomes, M.; Azevedo, H.; Malafaya, P.; Silva, S.; Oliveira, J.; Silva, G.; João Mano, R. S.; Reis, R. Natural Polymers in Tissue Engineering Applications A2. In *Handbook of Biopolymers and Biodegradable Plastics*; William Andrew Publishing: Boston, 2013; pp 385–425.
- (36) Averous, L. Biodegradable multiphase systems based on plasticized starch: a review. *J. Macromol. Sci., Polym. Rev.* **2004**, *44* (3), 231–274.
- (37) Robert, J.; Young, P. A. L. *Introduction to Polymers*, 3rd ed.; CRC Press: Florida, U.S.A., 2011; pp 591–622.
- (38) Hautamäki, M.; Meretoja, V. V.; Mattila, R. H.; Aho, A. J.; Vallittu, P. K. Osteoblast response to polymethyl methacrylate bioactive glass composite. *J. Mater. Sci.: Mater. Med.* **2010**, *21* (5), 1685–1692.
- (39) Mousa, W. F.; Kobayashi, M.; Shinzato, S.; Kamimura, M.; Neo, M.; Yoshihara, S.; Nakamura, T. Biological and mechanical properties of PMMA-based bioactive bone cements. *Biomaterials* **2000**, *21* (21), 2137–2146.
- (40) Vergnol, G.; Ginsac, N.; Rivory, P.; Meille, S.; Chenal, J.-M.; Balvay, S.; Chevalier, J.; Hartmann, D. J. In vitro and in vivo evaluation of a polylactic acid-bioactive glass composite for bone fixation devices. *J. Biomed. Mater. Res., Part B* **2016**, *104* (1), 180–191.
- (41) Raynaud, S.; Champion, E.; Bernache-Assollant, D.; Thomas, P. Calcium phosphate apatites with variable Ca/P atomic ratio I. Synthesis, characterisation and thermal stability of powders. *Biomaterials* **2002**, *23* (4), 1065–1072.
- (42) Thangakumaran, S.; Sudarsan, S.; Arun, K.; Talwar, A.; James, J. R. Osteoblast response (initial adhesion and alkaline phosphatase activity) following exposure to a barrier membrane/enamel matrix derivative combination. *Indian J. Dent. Res.* **2009**, *20* (1), 7.
- (43) Zhong, X.; Dehghani, F. Fabrication of biomimetic poly-(propylene carbonate) scaffolds by using carbon dioxide as a solvent, monomer and foaming agent. *Green Chem.* **2012**, *14* (9), 2523–2533.
- (44) Wang, Y.; Zhao, Z.; Zhao, B.; Qi, H.; Peng, J.; Zhang, L.; Xu, W.; Hu, P.; Lu, S. Biocompatibility evaluation of electrospun aligned poly (propylene carbonate) nanofibrous scaffolds with peripheral nerve tissues and cells in vitro. *China Med. J.* **2011**, *124* (15), 2361–2366.
- (45) Halasz, K.; Csoka, L. Plasticized Biodegradable Poly(lactic acid) Based Composites Containing Cellulose in Micro- and Nanosize. *J. Eng.* **2013**, *2013*, 9.
- (46) Wan, P.; Yuan, C.; Tan, L. L.; Li, Q.; Yang, K. Fabrication and evaluation of bioresorbable PLLA/magnesium and PLLA/magnesium fluoride hybrid composites for orthopedic implants. *Compos. Sci. Technol.* **2014**, *98*, 36–43.
- (47) Suganuma, J.; Alexander, H. Biological response of intramedullary bone to poly-L-lactic acid. *J. Appl. Biomater.* **1993**, *4* (1), 13–27.
- (48) Jimi, E.; Hirata, S.; Osawa, K.; Terashita, M.; Kitamura, C.; Fukushima, H. The Current and Future Therapies of Bone Regeneration to Repair Bone Defects. *Int. J. Dent.* **2012**, *2012*, 7.
- (49) Tal, H.; Kozlovsky, A.; Nemcovsky, C.; Moses, O. *Bioresorbable Collagen Membranes for Guided Bone Regeneration*; INTECH Open Access Publisher, 2012.